Proceedings of the 10th World Congress on Recent Advances in Nanotechnology (RAN 2025)
Barcelona, Spain - April, 2025
Paper No. ICNNFC 131
DOI: 10.11159/icnnfc25.131

Organometallic Synthesis Applied To Pt-Based Nanocatalysts for Oxygen Reduction Reaction

Nargiz Kazimova[1], Nuria Romero[1], Carlos A. Campos-Roldán[2], Marjorie Cavarroc[3], Sara Cavaliere[2], Karine Philippot[1]
[1] LCC-CNRS, University of Toulouse
205 Route de Narbonne, 31400, Toulouse, France
nargiz.kazimova@lcc-toulouse.fr; nuria.romero@lcc-toulouse.fr; karine.philippot@lcc-toulouse.fr
[2] ICGM, Univ. Montpellier, CNRS, ENSCM
1919 Route de Mende, 34293, Montpellier, France
carlos-augusto.campos-roldan@umontpellier.fr; sara.cavaliere@umontpellier.fr
[3] Safran-Tech, Materials and Processes Department
Rue des jeunes Bois, 78114, Magny-Les-Hameux, France
marjorie.cavarroc@safrangroup.com

Abstract – The need for sustainable energy technologies increased with fossil fuel depletion and atmosphere-pollution issues. For this concern, proton exchange membrane fuel cells (PEMFCs) stand out for their high conversion efficiency and low environmental pollution. As Pt-based catalysts are known as the most effective for the oxygen reduction reaction (ORR) that occurs at the PEMFC cathode, it is essential to enhance their catalytic efficiency and reduce the costs in view of commercializing fuel cell technology. Our work focuses on synthesizing carbon-supported Pt-based nanoparticles (NPs) using a solution organometallic chemistry approach to have control over the composition, structure and morphology of the NPs. Two distinct synthesis pathways have been used for studying their influence on the electrocatalytic activity of the obtained nanomaterials.

***Keywords*:** platinum, nanocatalysts, solution organometallic synthesis, oxygen reduction reaction (ORR), fuel cell.

1. Introduction

Fossil fuels depletion and environmental pollution raise an urgent need in developing efficient technologies for the sustainable energy production, conversion, and storage in both academia and industry. Proton exchange membrane fuel cells (PEMFCs) are among the most promising technologies, due to their high conversion efficiency and low environmental pollution.[1] However, a significant PEMFC limitation is the sluggish kinetics of electrocatalytic reduction of oxygen in the acidic environment at the cathode, leading to a large overpotential loss under typical hydrogen fuel cell operating conditions. Nowadays, Pt-based catalysts demonstrate the best electrocatalytic activity for the cathodic oxygen reduction reaction (ORR). Metal nanoparticles (MNPs) have a high surface-to-volume ratio and low-coordinated and high-energy atoms. The synthesis of MNPs can be achieved by various physical and chemical techniques. [2], [3] Among the bottom-up syntheses, the organometallic approach offers high versatility to control size, shape, composition and structure of the nanomaterials, by playing with the nature of organometallic precursors and stabilizers, the tuning of temperature and pressure.[4] Here we describe the synthesis of Pt-based nanocatalysts using the tris(norbornene)platinum, $[Pt(NBE)_3]$, organometallic precursor and hexadecylamine (HDA) as a stabilizer and EC 300J KetjenBlack Carbon (KB) as a support and their evaluation in ORR in acidic conditions.

2. Materials and Methods

All syntheses were carried out using Fisher–Porter reactors, a glove-box (Braun, <1 ppm H_2O, <1 mmol O_2) and argon-vacuum line techniques. Ar (≥99.999%) and H_2 (≥99.999%) were purchased from Air Liquide Solvents (toluene, pentane) and purified on a MBraun SPS-800 solvent purification system and then degassed by freeze-pump-thaw method. $[Pt(NBE)_3]$ was purchased from Nanomeps, hexadecylamine (HDA) from Sigma-Aldrich, and 30% Pt/C Benchmark from Johnson Matthey Technology Center. All reactants were used as received.

Transmission electron microscopy (TEM) analyses were performed using a JEOL JEM 1400 microscope operating at 120 kV with a point resolution of 2.0 Å. Colloidal solutions were drop-casted onto carbon-coated copper grids and dried under vacuum for one day. Particle mean size and size distribution were obtained by manual measurement of at least 100 particles, using ImageJ software.

Pt content was determined by inductively coupled plasma optical emission spectroscopy (ICP-OES) on a Thermo Scientific ICAP 6300 instrument after dissolving the samples in HCl : HNO_3 (3 : 1 v/v) mixture and dilute with MilliQ water.

Electrochemical activity towards ORR was investigated using a rotating-disk electrode (RDE) in a typical 3-electrodes cell connected to an electrochemical workstation BioLogic Potentiostat SP-300 equipped with a reversible hydrogen electrode (RHE) as reference electrode and a graphitic rod as counter electrode. Rotating Disk Glassy carbon electrode (RDE) was polished to a mirror finish with Al slurries, and sonicated in isopropanol and Milli-Q water to remove polishing residues. The catalyst inks were prepared by dispersing 3.4 mg of nanocatalyst in a mixture of 1 mL of isopropanol, 20 µL of 5% Nafion in isopropanol, and 3.98 mL of Milli-Q water [7]. Then, 20 µL of each suspension were deposited on the glassy carbon electrode with geometric area of 0.196 cm^2 followed by the electrode drying by rotation at 350 rpm. The nanocatalyst loading resulted in 20 μg_{Pt} $cm^{-2}{}_{geo}$. Cyclic voltammograms (CV) were recorded in N_2-saturated 0.1 M $HClO_4$ electrolyte at 20 $mV \cdot s^{-1}$ (Figure 2a). Oxygen reduction reaction curves were recorded in O_2-saturated environment in 0.1 M $HClO_4$ (at 20 mV s^{-1} and 1600 rpm) using a glassy carbon rotating disk electrode (RDE) (Figure 2b). ECSA were determined from H_2 desorption region of the CV graphs (Table 1 and Figure 2a). The ECSA was calculated from the normalization of Pt surface (S_{Pt}) to the Pt loading (L_{Pt}) as reported previously.[6], [7] Mass activities (I_m) were calculated at 0.9 V/RHE relative to the Pt loading (L_{Pt}) and specific activities (I_s) relative to the Pt surface (S_{Pt}) [5], [6] and given in Table 1.

3. Results

3.1. Synthesis of Pt NPs and impregnation onto carbon support

A toluene solution of $[Pt(NBE)_3]$ and HDA ([Pt]/[HDA]=1/1 was exposed to 3 bar of hydrogen under magnetic stirring at -10°C for 10 min and then at RT for 16 h. The obtained Pt colloidal suspension contains 4.9 ± 0.6 nm Pt NPs as shown by transmission electron microscopy (TEM) analysis (Figure 1a). Then, the obtained Pt NPs colloidal suspension was transferred onto a toluene suspension of KetjenBlack EC 300J (KB) carbon which is used as a support. The mixture was stirred at RT for 5 days. The solid material was easily isolated by decantation, the supernatant was removed by cannula and the solid was washed several times with pentane to eliminate unsupported Pt NPs. TEM analysis of the purified material (Pt-KB-I) redispersed in toluene (Figure 1b) showed well-dispersed NPs on the KB support with a size of 5.5 ± 0.7 nm close to that of the initial Pt NPs (4.9 ± 0.6 nm). EA and ICP data indicated a 28.8 wt% of Pt on carbon. As an alternative preparation protocol, the $[Pt(NBE)_3]$ complex was exposed to hydrogen in the presence of HDA and KB carbon, keeping all the other reaction parameters the same (toluene, ([Pt]/[HDA]=1/1, 3 bar of H_2, at -10°C for 10 min then R.T. for 16 h) and the same purification treatment (pentane washing and drying under vacuum), leading to Pt/KB-D nanomaterial. EA and ICP data indicated a 28.6 wt% of Pt that is very similar to that of the two-step prepared Pt/KB-I. TEM analysis showed very well-dispersed Pt NPs on the KB carbon (Figure 1c). However, in this case a size of 2.3 ± 0.4 nm was measured for the Pt NPs that is significantly lower than for the Pt/KB-I nanomaterial (5.5 ± 0.7 nm). This lower size can owe to the presence of KB carbon from the initial step of reaction as it may contribute to the Pt NP stabilization from the early stage of their formation and thus limit their growth.

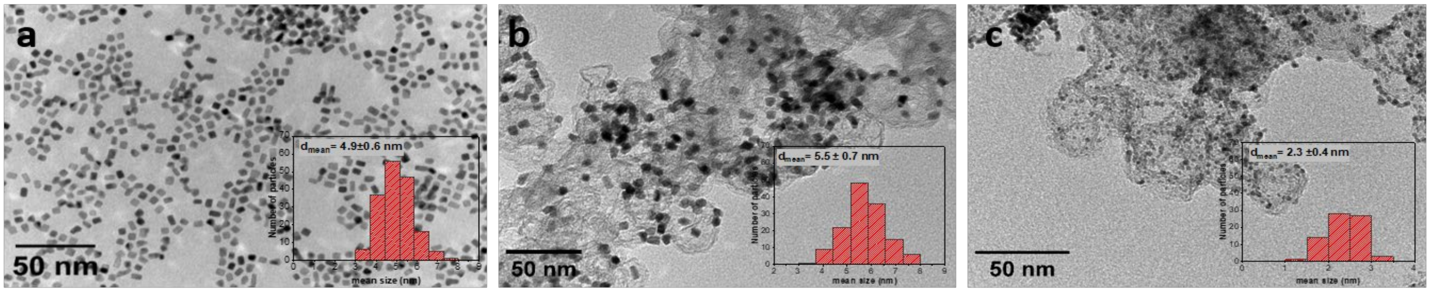

Figure 1. TEM images of unsupported Pt NPs (a), KB-supported Pt NPs prepared by a two-step C (Pt/KB-I) (b) and a one-step (Pt/KB-D) (c) protocol.

3.2. Electrochemical characterization

Electrochemical studies were conducted on the two Pt nanomaterials described above (Pt/KB-I and Pt/KB-D) plus a commercial Pt/C reference of similar metal loading (30% wt. Pt/C JM). Cyclic voltammograms (CV) and oxygen reduction reaction (ORR) polarization curves are shown in Figure 2a-b. Figure 2c displays the mass transport-corrected ORR polarization curves and normalized by Pt mass. The results indicate that the electrochemical surface area (ECSA) value of the one-step synthesized nanocatalyst (Pt/KB-D) is significantly higher than that of its counterpart prepared by impregnation of KB with preformed Pt NPs (Pt/KB-I) (Table 1). Several hypotheses can explain this difference: 1) Pt NP sizes are different (4.9 nm for Pt/KB-I *vs* 2.3 nm for /Pt/KB-D, respectively), 2) different surface chemistry, as the HDA stabilizer can be differently coordinated to the Pt NPs, 3) different interaction of the Pt NPs with the carbon support. Owing to the lower size of the Pt NPs directly grown on the KB, this latter may contribute to their stabilization which can lead to a better interaction between the two and so promote a more efficient electron transfer, resulting in a higher ORR activity. On the ORR voltammetry (Figure 2b), a steep reduction wave is observed for samples deposited on carbon in the mixed kinetic-diffusion region (0.75 V to 1 V) and diffusion limited current density plateau is flat and the steady (0.2 V to 0.7 V), indicating efficient oxygen transport to the electrode. The electrocatalytic activity of the different supported catalysts is compared based on calculated mass (I_m) and specific activity $(I)_s$ at 0.9 V/RHE (Table 1). The I_m values is higher for Pt/KB-D than for Pt/KB-I. However, for I_s, the trend is reversed. This may be explained due to the more accessible active sites of Pt/KB-I catalyst, with a low intrinsic activity and low ECSA. In contrast, Pt/KB-D catalyst seems to have fewer active sites exposed but higher intrinsic catalytic properties. As a result, the catalyst from direct synthesis can achieve the same catalytic activity than the reference with a smaller mass of material compared to the one obtained by a two-step method, making it a promising candidate for further development.

Table 1. ECSA and ORR kinetic parameters of Pt nanomaterials.

Nanocatalyst	ECSA ($m^2_{pt}g_{pt}^{-1}$)	I_s (mA cm^{-2}_{Pt}) @ 0.9 V/RHE	I_m (A/mg_{Pt}) @ 0.9 V/RHE
Pt/KB-I	9.7	1.3	0.1
Pt/KB- D	39.5	0.8	0.3
Pt/C Benchmark	56.6	0.8	0.4

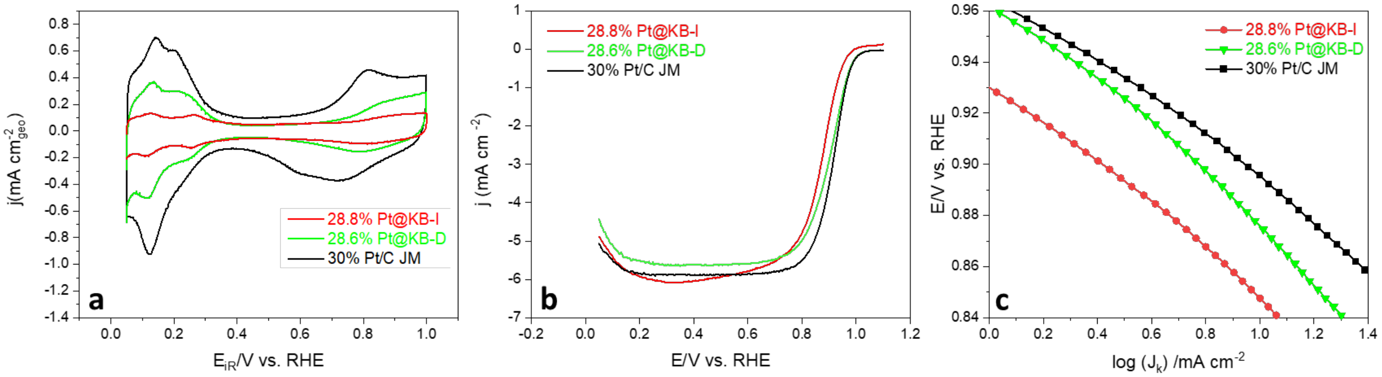

Figure 2. a) Cyclic voltammograms (CV) in N_2- saturated 0.1 M $HClO_4$ at 20 mV s^{-1}, b) ORR polarization curves in O_2- saturated 0.1 M $HClO_4$ at 20 mV s^{-1} at 1600 rpm, c) Mass-transport corrected ORR polarization curves.

4. Conclusion

The organometallic synthesis approach allowed to easily prepare carbon-supported Pt NPs in mild conditions via two different methods. The impregnation of carbon support with a colloidal suspension of pre-stabilized Pt NPs led to nanomaterial with quite-well dispersed 5.5 nm in size Pt NPs. The direct synthesis in the presence of carbon support and hexadecylamine as stabilizer led to Pt NPs with a smaller size (2.3 nm) and a better dispersion. The differences in size and dispersion as well as a better interaction between Pt and carbon support can explain the higher ORR performance observed for the one-step synthesized nanocatalyst. Our results validate the organometallic synthesis approach as a promising direction for achieving nanocatalysts of significant attractivity for electrocatalytic applications such as the functionalization of cathodes of fuel cells.

Acknowledgements

We would like to thank CNRS, RhyO, Region Occitanie and SAFRAN for funding this project. We thank also A. Moreau for ICP analyses and I. Borget for Elemental analysis. Centre of Micro characterization Raimond Castaing, CNRS-UAR 3623, is acknowledged.

References

[1] X. Tang, D. Fang, L. Qu, D. Xu, X. Qin, W. Song, Z. Shao and B. Yi, “Carbon-supported ultrafine Pt nanoparticles modified with trace amounts of cobalt as enhanced oxygen reduction reaction catalysts for proton exchange membrane fuel cells,” Chinese Journal of Catalysis, vol. 40, no. 4, pp. 504–514, 2019.

[2] A. F. Burlec, A. Corciova, M. Boev, D. Batir-Marin, C. Mircea, O. Cioanca, G. Danila, M. Danila, A. F. Bucur, and M. Hancianu, “Current Overview of Metal Nanoparticles’ Synthesis, Characterization, and Biomedical Applications, with a Focus on Silver and Gold Nanoparticles,” Pharmaceuticals, vol. 16, no. 10, Art. no. 10, 2023.

[3] B. L. Cushing, V. L. Kolesnichenko, and C. J. O’Connor, “Recent Advances in the Liquid-Phase Syntheses of Inorganic Nanoparticles,” Chem. Rev., vol. 104, no. 9, pp. 3893–3946, 2004.

[4] M. R. Axet and K. Philippot, “Organometallic Metal Nanoparticles for Catalysis,” in Nanoparticles in Catalysis, K. Philippot and A. Roucoux, Eds., Wiley, 2021, pp. 73–97.

[5] Y. Garsany, O. A. Baturina, K. E. Swider-Lyons, and S. S. Kocha, “Experimental Methods for Quantifying the Activity of Platinum Electrocatalysts for the Oxygen Reduction Reaction,” Anal. Chem., vol. 82, no. 15, pp. 6321–6328, 2010.

[6] K. J. J. Mayrhofer, D. Strmcnik, B. B. Blizanac, V. Stamenkovic, M. Arenz, and N. M. Markovic, “Measurement of oxygen reduction activities via the rotating disc electrode method: From Pt model surfaces to carbon-supported high surface area catalysts,” Electrochimica Acta, vol. 53, no. 7, pp. 3181–3188, 2008.

[7] C. A. Campos-Roldán, F. Pailloux, P.-Y. Blanchard, D. J. Jones, J. Rozière, and S. Cavaliere, “Rational Design of Carbon-Supported Platinum–Gadolinium Nanoalloys for Oxygen Reduction Reaction,” ACS Catal., vol. 11, no. 21, pp. 13519–13529, 2021.